

# Appendix of “Superpixel Segmentation based Evolutionary Multitasking Algorithm for Feature Selection of Hyperspectral Images”

Lingjie Li, *Member, IEEE*, Yuze Zhang, Qiuzhen Lin, *Member, IEEE*, Zhong Ming, Carlos A. Coello Coello, *Fellow, IEEE*, and Victor. C. M. Leung, *Life Fellow, IEEE*

## S-I. DETAILS OF DATASETS

(Please read first Section IV. A of the paper.)

This section presents the details of all the adopted datasets in our experiments, which are as follows:

- **Indian Pines:** The Indian Pines dataset is considered the earliest test dataset for hyperspectral image classification, which was imaged by the Airborne Visible Infrared Imaging Spectrometer (AVIRIS) in 1992 on a patch of Indian Pines in Indiana, USA, and then intercepted at a size of  $145 \times 145$  for annotation with the purpose for hyperspectral image classification test. The AVIRIS imaging spectrometer images wavelengths in the range of  $0.4\text{--}2.5\mu\text{m}$ , and the Indian pine landscape contains two-thirds agriculture and one-third forest or other natural perennial vegetation. There are two major two-lane highways, a railway line, and some low-density housing, other built structures, and smaller roads. Since the scene was shot in June, some crops, corn, and soybeans are in the early stages of growth. The cover is less than 5%, and the available basic facts are assigned to 16 classes. The number of bands is reduced to 200 after removing the bands covering the water absorption area.
- **Pavia University:** The Pavia University dataset was acquired by the ROSIS sensor in 2002 and is often used for hyperspectral image classification. The sensor has a total of 115 bands and a size of  $610 \times 610$  pixels. This dataset discarded some uninformative samples before further analysis, and after processing, the Pavia University dataset has 103 bands with a size of  $610 \times 340$  pixels. The geometric resolution is 1.3 meters and the images have 9 classes.
- **Salinas:** The Salinas dataset was acquired by the VIRIS sensor at 224-band AVIRIS over the Salinas Valley, California, USA, and is characterized by a high spatial resolution (3.7 meter pixels). The area covered includes 512 lines by 217 samples. As with the Indian pine scene, 20 absorption bands were discarded. The image is available only as radiometric data at the sensor. It includes 16 classes of vegetables, bare soil and vineyards, among others.
- **Botswana:** The Botswana dataset is a series of data acquired by the Hyperion sensor on board the NASA EO-1 satellite over the Okavango Delta in Botswana in 2001-2004 at 30 m pixel resolution over a 7.7 km strip. 242

bands in the 10 nm window covering the 400-2500 nm portion of the spectrum. Preprocessing of the data was performed by the UT Space Research Center to mitigate the effects of bad detectors, inter-detector calibration errors, and intermittent anomalies. The remaining 145 bands are included as candidate features by removing the uncalibrated and noisy bands covering the absorption features. Observations from 14 classes are included.

Furthermore, Fig. S-1 provides the ground-truth maps and the feature classes contained in the Indian Pines, Pavia University, Salinas, and Botswana datasets, respectively.

## S-II. INTRODUCTION OF PERFORMANCE METRICS

(Please read first Section IV. A of the paper.) This section presents the details of the two performance metrics adopted in the experiments, i.e., overall accuracy (OA) and KAPPA coefficient, which are defined as follows:

1) Overall accuracy (OA): It is defined as:

$$OA = \frac{CP}{TP}, \quad (\text{S-1})$$

where  $CP$  denotes the number of correctly classified pixels and  $TP$  denotes the total number of pixels.

2) KAPPA coefficient: It is defined as:

$$KAPPA = \frac{Pr(o) - Pr(e)}{1 - Pr(e)}, \quad (\text{S-2})$$

with

$$Pr(o) = OA, \quad (\text{S-3})$$

$$Pr(e) = \frac{a_1 \times b_1 + a_2 \times b_2 + \dots + a_n \times b_n}{n \times n}, \quad (\text{S-4})$$

where  $Pr(e)$  is the hypothetical probability of chance agreement. It is assumed that there are  $n$  classes of features' information.  $\{a_1, a_2, \dots, a_n\}$  denote the number of real samples in each category of features information,  $\{b_1, b_2, \dots, b_n\}$  denote the number of samples in each type of features information in the prediction result.

## S-III. EXPERIMENTAL RESULTS

### A. Supplementary Materials for Section IV.D

(Please read first Section IV. D of the paper.) Table S-2 provides the parametric analysis results on *rmf*. Note that more detailed discussions can be read in Section IV. D of the paper.



Fig. S-1: The ground-truth maps of the (a) Indian Pines, (b) Pavia University, (c) Salinas, and (d) Botswana datasets.

TABLE S-1: Parameter Settings for the Compared Algorithms

Method	Parameter settings			
MVPCA	-			
EFDPC	-			
MOBS	-			
SSGA	$P_c = 0.9, P_{m1} = 0.02, P_{m2} = 0.1$			
MTPSO	$c_1 = c_2 = 1.49445, \omega = 0.9 - 0.5 * (iter/max\_iter), rmp = 0.6, G = 6$			
MBBS-VC	$K = 30, m = 5, u = 5$			
SS-EMT	$SP_N = 5, rmp = 0.5, c_1 = c_2 = c_3 = 1.49445, \omega = 0.9 - 0.5 * (t/Gmax)$			
	Indian Pines	Pavia University	Salina	Botswana
ASPS-MN	$B = 3, M = 10\%$	$B = 10, M = 10\%$	$B = 10, M = 10\%$	$B = 10, M = 10\%$
FNGBS	$k = 2, Z = 10\%$	$k = 3, Z = 1\%$	$k = 3, Z = 1\%$	$k = 2, Z = 1\%$
SSGA	$SP_N = 300$	$SP_N = 700$	$SP_N = 500$	$SP_N = 500$
SS-EMT	$J = 32$	$J = 18$	$J = 32$	$J = 28$

## B. Supplementary Materials for Section IV.E

### (Please read first Section IV. E of the paper.)

1) *Results on the Pavia University dataset:* Fig. S-2 and Fig. S-3 provide the OA and KAPPA coefficient results of SS-EMT and four non-EA compared methods on the Pavia University dataset under three different classifiers (KNN, SVM and RF), respectively. Note that more detailed discussions can be read in Section IV.E of the paper.

2) *Results on the Salinas dataset:* Fig. S-4 and Fig. S-5 provide the OA and KAPPA coefficient results of SS-EMT and four non-EA comparison methods on the Salinas dataset under

three different classifiers (KNN, SVM and RF), respectively. Note that more detailed discussions can be read in Section IV.E of the paper.

3) *Results on the Botswana dataset:* The OA results of each compared algorithm on the Botswana dataset are shown in Fig. S-6. From these figures, several conclusions can be drawn. First, SS-EMT achieves the best results on subsets of band sizes 3 to 30, which are significantly better than those of its four competitors. Fig. S-6(a) provides the OA results obtained using the KNN classifier. In particular, SS-EMT outperforms the baseline approach in most cases, except for the cases of 2 to 4 bands. However, most of the com-

TABLE S-2: Parametric analysis on *rm*p

Classifier	rm	2	4	6	8	10	12	14	16	18	20	22	24	26	28	30	Mean
KNN	0.1	<b>77.10</b>	<b>86.80</b>	88.90	89.65	90.15	90.80	90.92	<b>91.34</b>	91.31	91.44	91.52	91.65	91.85	91.77	91.78	89.80
	0.3	63.27	81.55	86.98	88.96	89.96	90.18	90.70	90.82	91.19	91.32	91.39	91.31	91.48	91.48	91.60	88.15
	0.5	75.22	86.57	<b>89.05</b>	<b>90.02</b>	<b>90.77</b>	<b>91.07</b>	<b>91.23</b>	91.28	<b>91.58</b>	<b>91.63</b>	<b>91.73</b>	<b>91.66</b>	<b>91.87</b>	<b>92.03</b>	<b>91.84</b>	<b>89.84</b>
	0.7	68.26	82.67	86.57	88.64	89.72	90.33	90.89	91.11	91.16	91.25	91.40	91.57	91.61	91.56	91.84	88.57
	0.9	64.19	78.50	84.04	87.29	88.76	89.48	90.05	90.50	90.84	90.97	91.07	91.29	91.29	91.31	91.53	87.41
SVM	0.1	64.39	<b>86.23</b>	89.61	91.04	91.68	92.27	92.51	92.82	93.00	92.98	93.18	93.19	93.22	93.51	<b>93.53</b>	90.21
	0.3	57.24	80.31	87.64	90.14	91.51	92.06	92.36	92.61	92.91	93.00	93.21	93.26	93.27	<b>93.55</b>	93.34	89.09
	0.5	<b>65.86</b>	85.61	<b>89.76</b>	<b>91.34</b>	<b>92.32</b>	<b>92.78</b>	<b>92.75</b>	<b>92.82</b>	<b>93.25</b>	<b>93.18</b>	93.20	<b>93.54</b>	<b>93.55</b>	93.44	93.51	<b>90.46</b>
	0.7	62.79	81.98	87.31	90.15	91.18	91.91	92.64	92.70	92.80	92.93	<b>93.27</b>	93.32	93.19	93.42	93.43	89.54
	0.9	58.94	77.68	84.51	88.68	90.40	91.57	92.12	92.27	92.58	92.84	93.08	93.08	92.99	93.20	93.21	88.48
RF	0.1	<b>76.51</b>	<b>87.40</b>	89.13	89.83	90.41	90.81	90.93	91.19	91.37	91.51	<b>91.83</b>	91.74	91.81	<b>91.98</b>	92.03	<b>89.90</b>
	0.3	63.15	82.27	87.42	89.23	90.22	90.61	90.96	91.13	91.47	91.68	91.64	<b>91.88</b>	91.79	91.75	<b>92.06</b>	88.48
	0.5	74.58	86.55	<b>89.13</b>	<b>90.09</b>	<b>90.87</b>	<b>91.21</b>	<b>91.19</b>	<b>91.46</b>	<b>91.76</b>	<b>91.71</b>	91.62	91.85	<b>91.91</b>	91.92	92.01	89.86
	0.7	67.68	83.31	86.99	88.97	90.02	90.48	91.03	91.22	91.28	91.32	91.71	91.80	91.71	91.89	91.88	88.75
	0.9	63.73	78.91	84.47	87.51	89.03	89.74	90.27	90.53	91.04	91.12	91.48	91.57	91.64	91.58	91.68	87.62

pared algorithms are unable to achieve better classification results than the baseline approach. Second, the classification results of SS-EMT can exceed 94% with only a subset of 15 bands, while the classification results of the other compared algorithms are only between 75% and 88% in the same situation. In addition, Figs. S-6(b)-(c) show the OA results of each compared algorithm using the SVM and RF classifiers, respectively, which also obtained similar results. Finally, as shown in Fig. S-6(d), the average OA of SS-EMT is much higher than that of the others. In summary, Fig. S-6 verifies that the proposed SS-EMT outperforms these four competitors in terms of the OA results obtained under the KNN, SVM and RF classifiers.

Furthermore, Fig. S-7 shows the KAPPA coefficient results for each compared algorithm on the Bostwana dataset under three different classifiers, further confirming the superiority of our proposed SS-EMT over these four non-EA-based FS methods. In order to visualize the results, Figs. S-14 to S-16 respectively show the classification maps for non-EA-based FS methods on the Pavia University, Salinas, and Botswana datasets, respectively. These classification results on different HSI datasets show that the classification maps of SS-EMT are much clearer than those of other non-EA-based algorithms.

### C. Supplementary Materials for Section IV.F

(Please read first Section IV. F of the paper.)

1) *Results on the Pavia University dataset:* Fig. S-8 and Fig. S-9 provide the OA and KAPPA coefficient results of SS-EMT and four compared EA-based FS methods on the Pavia University dataset under three different classifiers (KNN, SVM and RF), respectively. Note that more detailed discussions can be read in Section IV.F of the paper.

2) *Results on the Salinas dataset:* Fig. S-10 and Fig. S-11 provide the OA and KAPPA coefficient results of SS-EMT and four compared EA-based FS methods on the Salinas dataset under three different classifiers (KNN, SVM and RF), respectively. Note that more detailed discussions can be read in Section IV.F of the paper.

3) *Results on the Bostwana dataset:* Fig. S-12 shows the OA results for the Bostwana dataset. Some conclusions can be drawn from these figures. First, compared to the other four EA-based FS methods, SS-EMT achieves the best results under all three classifiers on subsets with 3 to 30 bands. Second,

SS-EMT outperforms the baseline approach in most cases. None of the compared algorithms outperformed the baseline approach even on a subset with 30 bands. Furthermore, as shown in Fig. S-12(d), the average results of the four EA algorithms are relatively close, but the average OA results of all compared algorithms are much lower than those of our proposed SS-EMT. Therefore, Fig. S-12 validates the effectiveness and superiority of SS-EM.

In addition, Fig. S-13 shows the results of the KAPPA coefficients for each of the compared algorithms on the Botswana dataset under three different classifiers, which further confirms the superiority of our proposed SS-EMT over these four EA-based FS methods. In order to visualize the results, Figs. S-17 to S-20 respectively show the classification maps for EA-based FS methods on the Indian Pines, Pavia University, Salinas, and Botswana datasets. These classification results on different HSI datasets show that the classification maps of SS-EMT are much clearer than those of other EA-based algorithms.

### D. Supplementary Materials for Section IV.H

(Please read first Section IV. H of the paper.) In this section, we will further investigate the validity of two other important components of our approach, including the fitness function and the individuals' evaluation mechanism. To this end, two groups of ablation experiments were arranged as follows:

- To validate the effectiveness of the fitness function, we designed two variants of our approach, i.e., SS-EMT-I and SS-EMT-II. Specifically, SS-EMT-I replaces the original fitness function in our approach with variation coefficient [1] and mutual information, and SS-EMT-II adopts information entropy and spectral angle [2] as its fitness function. Table S-3 provides the OA results for our approach and these two variants on the IP dataset. Clearly, the experimental results show that our approach achieves a better performance than these two variants, which indicates that the adopted fitness function is more suitable for our approach.
- To validate the effectiveness of the individuals' evaluation mechanism, we devised a variant of our approach, namely SS-EMT w/o EM, which employs an independent individuals' evaluation mechanism for each subset of bands, as in previously existing work [3], [4]. Table S-4 provides

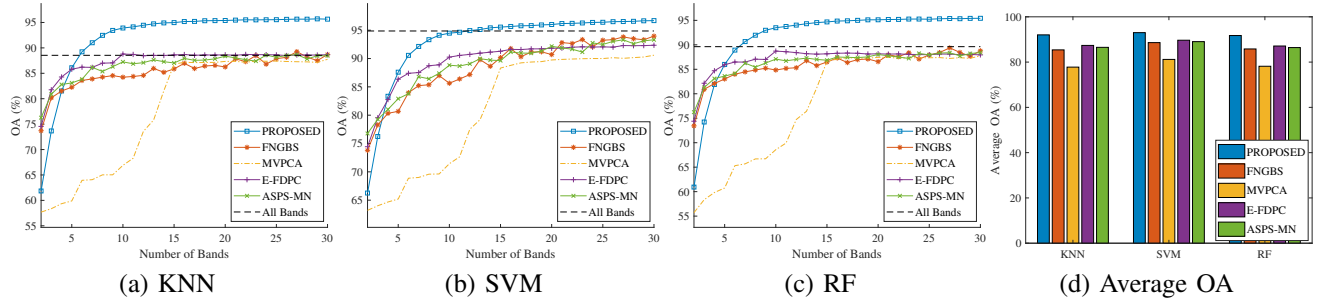


Fig. S-2: OA results of SS-EMT and four non-EA-based FS methods on the Pavia University dataset.

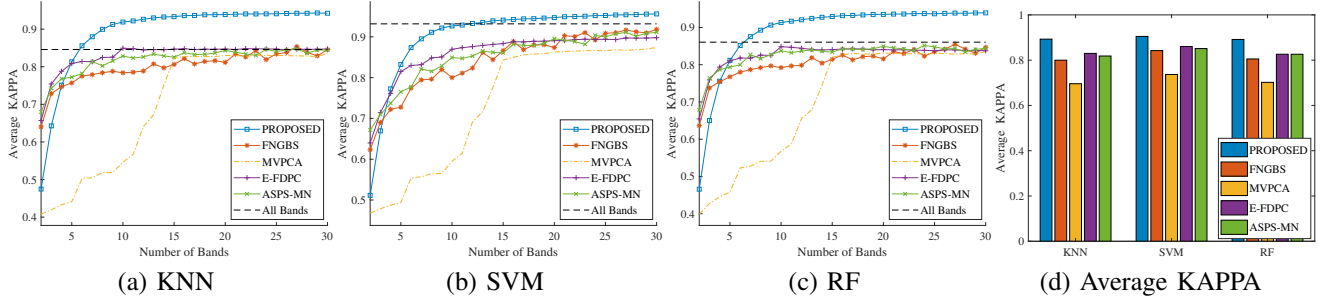


Fig. S-3: KAPPA coefficient results of SS-EMT and four non-EA-based FS methods on the Pavia University dataset.

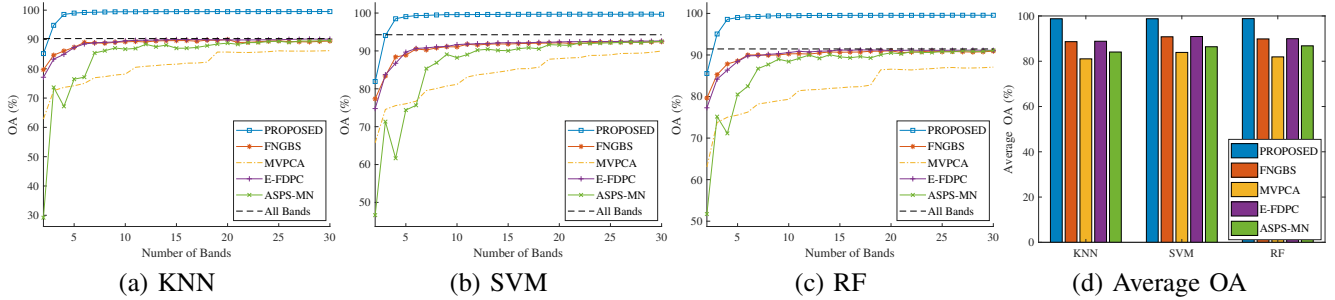


Fig. S-4: OA results of SS-EMT and four non-EA-based FS methods on the Salinas dataset.

the experimental results of our approach and SS-EMT w/o EM on four HSI datasets. As shown in Table S-4, the accuracy of our approach is almost identical to that of SS-EMT w/o EM that employs an independently and accurately evaluated mechanism for each band subset, but the time cost of our approach is much lower than that of SS-EMT w/o EM. Thus, the experimental results show that our designed individual evaluation mechanism is able to significantly reduce the time cost of band subset evaluation while preserving the accuracy.

### E. Particle Swarm Optimization

Particle swarm optimization (PSO) is a computational optimization technique that aims to find the optimal solution by simulating the movement and cooperation of particles in a multidimensional search space. In PSO, the population is considered as a swarm composed of particles, and each particle has two characteristics: 1) position and 2) velocity. For instance, at the  $t^{th}$  generation, the position of each particle

can be represented as follows:

$$X_i(t) = [x_{i,1}(t), x_{i,2}(t), \dots, x_{i,D}(t)], \quad (S-5)$$

where  $D$  represents the dimensionality of the search space (i.e., the number of bands in the HSI dataset), and  $i$  ranges from 1 to  $SP_N$ , where  $SP_N$  is the size of the particles. Additionally, each particle possesses a velocity, denoted as:

$$V_i(t) = [v_{i,1}(t), v_{i,2}(t), \dots, v_{i,D}(t)]. \quad (S-6)$$

At the  $t^{th}$  generation,  $X_{pbest_i}$  represents the personal best position for the  $i^{th}$  particle and  $X_{gbest}$  represents the global best position at the current iteration. Based on  $X_{pbest_i}(t)$  and  $X_{gbest_i}(t)$ , the velocity and position of the  $i^{th}$  particle in the next generation can be updated by equation (10) and equation (11) in Section III-C of the manuscript.

### F. Comparisons with Two Recent State-of-the-art Non-EA-based FS Methods

In this section, to further validate the efficiency of our proposed SS-EMT, we add an additional comparison with respect to two recent state-of-the-art non-EA-based FS methods,

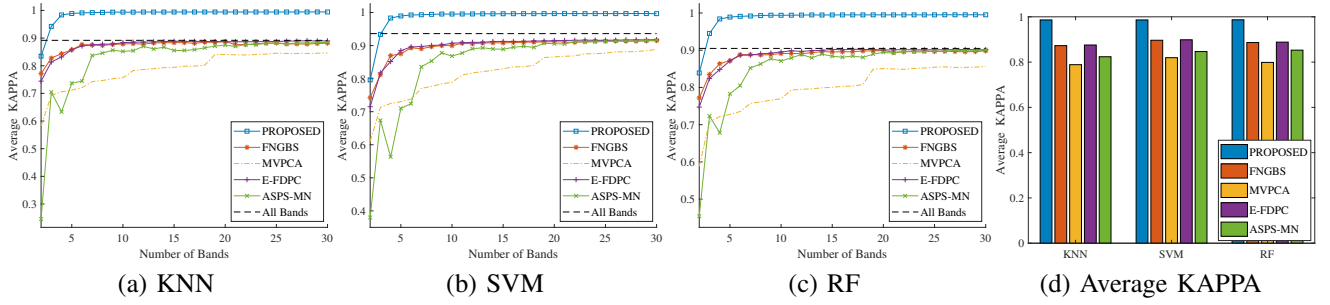


Fig. S-5: KAPPA coefficient results of SS-EMT and four non-EA-based FS methods on the Salinas dataset.

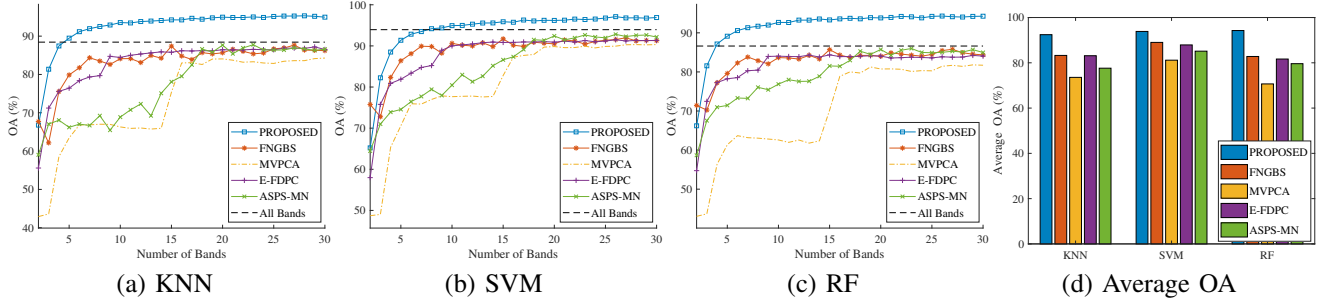


Fig. S-6: OA results of SS-EMT and four non-EA-based FS methods on the Bostwana dataset.

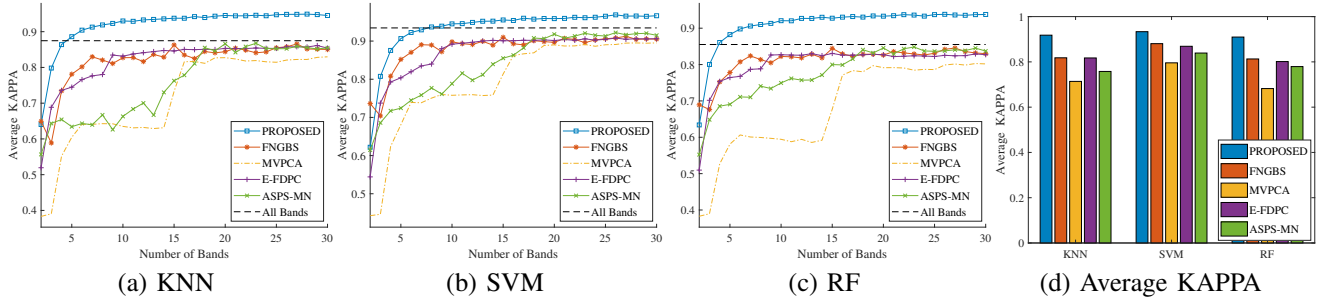


Fig. S-7: KAPPA coefficient results of SS-EMT and four non-EA-based FS methods on the Bostwana dataset.

TABLE S-3: Comparisons between SS-EMT and two variants on IP dataset.

Classifier	Variant	2	4	6	8	10	12	14	16	18	20	22	24	26	28	30	Mean
KNN	SS-EMT	<b>75.22</b>	86.57	<b>89.05</b>	90.02	<b>90.77</b>	<b>91.07</b>	<b>91.23</b>	91.28	91.58	<b>91.63</b>	<b>91.73</b>	91.66	91.87	<b>92.03</b>	91.84	<b>89.84</b>
	SS-EMT-I	58.72	82.95	86.97	<b>90.69</b>	90.20	90.98	90.98	<b>91.79</b>	91.76	90.98	90.89	91.01	<b>92.21</b>	91.91	<b>91.86</b>	88.26
	SS-EMT-II	62.81	<b>86.83</b>	88.17	90.42	90.62	90.72	90.98	91.19	<b>92.02</b>	91.24	91.25	<b>91.86</b>	91.85	91.34	91.23	88.83
SVM	SS-EMT	<b>65.86</b>	85.61	<b>89.76</b>	<b>91.34</b>	<b>92.32</b>	<b>92.78</b>	92.75	92.82	93.25	93.18	<b>93.20</b>	<b>93.54</b>	<b>93.55</b>	<b>93.44</b>	93.51	<b>90.46</b>
	SS-EMT-I	54.20	83.95	88.85	90.32	92.29	92.42	92.92	92.68	<b>93.82</b>	<b>93.23</b>	93.19	92.90	93.44	93.40	<b>93.80</b>	89.43
	SS-EMT-II	61.14	<b>85.70</b>	89.76	91.31	92.02	92.41	<b>92.98</b>	<b>93.24</b>	92.85	92.34	92.58	92.84	93.20	93.43	92.76	89.90
RF	SS-EMT	<b>74.58</b>	<b>86.55</b>	<b>89.13</b>	<b>90.09</b>	<b>90.87</b>	<b>91.21</b>	91.19	<b>91.46</b>	<b>91.76</b>	<b>91.71</b>	<b>91.62</b>	91.85	91.91	91.92	92.01	<b>89.86</b>
	SS-EMT-I	58.06	82.32	86.55	89.82	89.38	90.33	91.02	90.60	91.01	91.02	91.13	91.38	91.54	91.29	91.64	87.81
	SS-EMT-II	60.28	85.83	88.13	89.76	89.90	90.72	<b>91.30</b>	91.19	91.23	91.08	91.35	<b>91.99</b>	<b>91.92</b>	<b>92.29</b>	<b>92.21</b>	88.61

including a marginalized graph self-representation (MGSR) method [5] and a graph regularized spatial-spectral subspace clustering (GRSC) method [6]. Specifically, MGSR explores spatial information in different homogeneous regions through superpixel segmentation, while GRSC explores the spectral associations between all bands using a self-representation subspace clustering model and  $l_{2,1}$ -paradigm regularization.

Tables S-5 to S-6 provide the OA and KAPPA results obtained by our proposed SS-EMT and these two recent state-of-the-art non-EA-based FS methods, respectively. Obviously, our algorithm achieves very significant advantages over these

two other methods on all four datasets under three classifiers. Thus, the results presented in Tables S-5 to S-6 further validate the performance advantages of our proposed SS-EMT.

## REFERENCES

- [1] C. He, Y. Zhang, D. Gong, X. Song, and X. Sun, "A multi-task bee colony band selection algorithm with variable-size clustering for hyperspectral images," *IEEE Trans Evol Comput*, vol. 26, no. 6, pp. 1566–1580, 2022.
- [2] Q. Li, Y. Yuan, X. Jia, and Q. Wang, "Dual-stage approach toward hyperspectral image super-resolution," *IEEE Trans Image Process*, vol. 31, pp. 7252–7263, 2022.

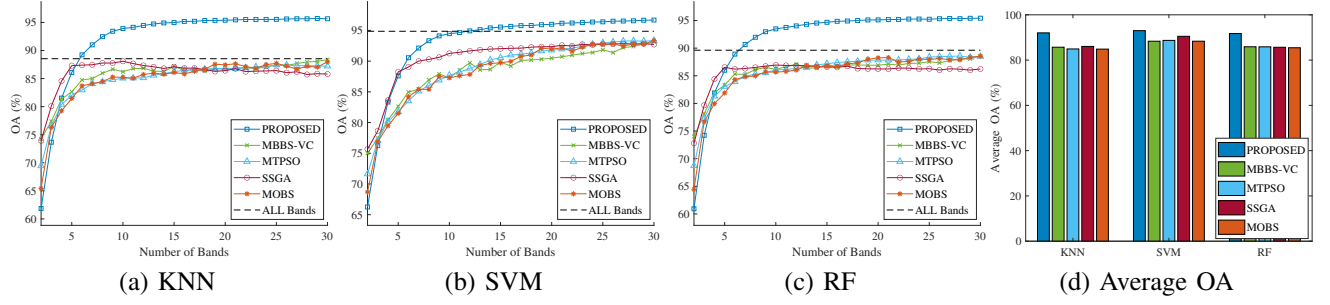


Fig. S-8: OA results of SS-EMT and four EA-based FS methods on the Pavia University dataset.

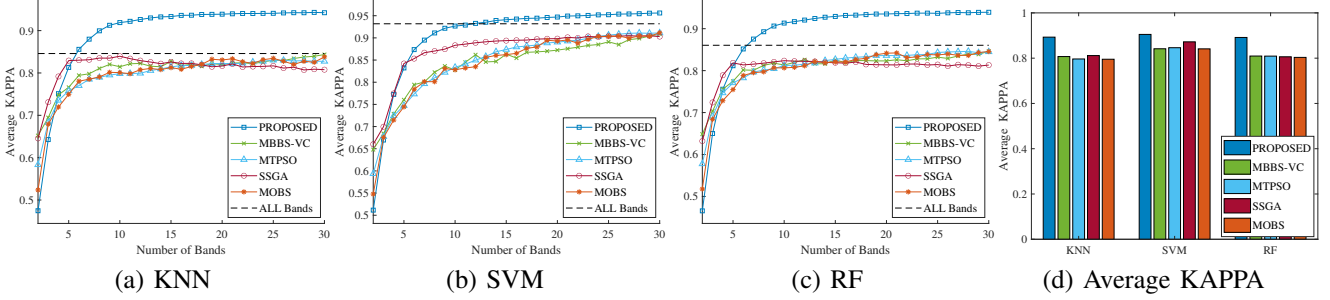


Fig. S-9: KAPPA coefficient results of SS-EMT and four EA-based FS methods on the Pavia University dataset.

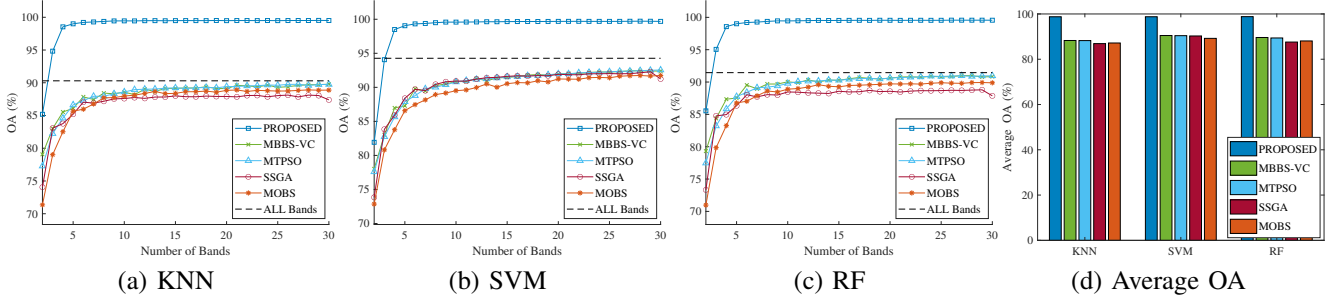


Fig. S-10: OA results of SS-EMT and four EA-based FS methods on the Salinas dataset.

TABLE S-4: Comparisons between SS-EMT and SS-EMT w/o EM on IP dataset.

Dataset	Variant	KNN	SVM	RF	TIME
IP	SS-EMT	89.91	90.21	89.97	321.37*
	SS-EMT w/o EM	<b>90.76</b>	<b>90.95</b>	<b>90.78</b>	1552.26
PU	SS-EMT	<b>93.30</b>	<b>94.02</b>	92.95	105.50*
	SS-EMT w/o EM	93.18	93.94	<b>93.43</b>	556.65
SA	SS-EMT	<b>99.31</b>	<b>99.43</b>	<b>99.34</b>	442.64*
	SS-EMT w/o EM	96.23	98.81	98.82	2023.62
BW	SS-EMT	92.46	93.71	91.88	336.21*
	SS-EMT w/o EM	<b>93.94</b>	<b>94.44</b>	<b>92.04</b>	2073.52

- [3] C. Chen, Y. Wan, A. Ma, L. Zhang, and Y. Zhong, "A decomposition-based multiobjective clonal selection algorithm for hyperspectral image feature selection," *IEEE Trans Geosci Remote Sens*, vol. 60, pp. 1–16, 2022. doi:10.1109/TGRS.2022.3216685.
- [4] Z. Yong, H. Chun-lin, S. Xian-fang, and S. Xiao-yan, "A multi-strategy integrated multi-objective artificial bee colony for unsupervised band selection of hyperspectral images," *Swarm Evol. Comput.*, vol. 60, p. 100806, 2021.
- [5] Y. Zhang, X. Wang, X. Jiang, and Y. Zhou, "Marginalized graph self-representation for unsupervised hyperspectral band selection," *IEEE Trans Geosci Remote Sens*, vol. 60, pp. 1–12, 2022.
- [6] J. Wang, C. Tang, X. Zheng, X. Liu, W. Zhang, and E. Zhu, "Graph regularized spatial-spectral subspace clustering for hyperspectral band selection," *Neural Networks*, vol. 153, pp. 292–302, 2022.

TABLE S-5: The OA results of SS-EMT and two recent state-of-the-art FS methods on four HSI datasets under three classifiers.

Dataset	Classifier	Algorithm	2	4	6	8	10	12	14	16	18	20	22	24	26	28	30	Mean
IP	KNN	SS-EMT	75.22	86.57	89.05	90.02	90.77	91.07	91.23	91.28	91.58	91.63	91.73	91.66	91.87	92.03	91.84	89.84
		GRSC	43.24	67.31	70.00	70.22	70.73	72.94	73.51	72.65	72.77	70.81	72.15	70.86	71.41	72.48	71.61	69.51
		MGSR	25.81	43.93	50.69	53.64	53.48	59.80	60.90	61.16	62.63	62.61	63.73	64.57	64.45	65.34	65.18	57.19
	SVM	SS-EMT	65.86	85.61	89.76	91.34	92.32	92.78	92.75	92.82	93.25	93.18	93.20	93.54	93.55	93.44	93.51	90.46
		GRSC	44.29	66.51	70.44	72.98	76.48	79.48	79.39	82.37	82.04	80.14	81.46	79.62	79.84	81.17	81.60	75.85
		MGSR	37.21	47.89	52.44	55.63	55.94	60.58	61.56	62.61	64.00	65.21	66.05	67.38	67.66	68.78	69.23	60.15
	RF	SS-EMT	74.58	86.55	89.13	90.09	90.87	91.21	91.19	91.46	91.76	91.71	91.62	91.85	91.91	91.92	92.01	89.86
		GRSC	43.51	68.71	69.73	70.69	73.04	73.79	73.51	75.23	73.54	73.35	75.04	73.85	74.44	73.63	74.97	71.32
		MGSR	27.84	45.98	53.05	55.86	55.10	60.53	60.79	61.67	62.12	62.52	62.50	63.68	63.64	63.89	64.86	57.60
PU	KNN	SS-EMT	62.52	88.52	93.15	94.42	94.87	95.20	95.33	95.47	95.50	95.61	95.73	95.77	95.83	95.84	95.87	92.64
		GRSC	67.33	83.55	84.48	86.38	87.58	85.55	86.12	87.47	88.52	88.27	88.44	88.68	88.71	87.97	89.22	85.84
		MGSR	68.64	72.07	74.11	76.02	78.84	82.80	83.45	85.75	85.94	86.06	87.59	88.34	88.25	88.36	88.17	82.29
	SVM	SS-EMT	66.11	89.14	93.90	94.97	95.27	95.45	95.72	95.83	96.06	96.24	96.38	96.51	96.64	96.75	96.92	93.46
		GRSC	71.35	83.24	84.71	88.11	90.10	89.62	90.46	91.67	92.04	92.54	92.63	92.55	92.62	92.75	93.12	89.17
		MGSR	72.76	75.02	76.26	78.71	81.04	84.88	85.67	86.82	86.98	87.56	88.92	89.46	89.77	89.78	89.77	84.23
	RF	SS-EMT	62.12	88.22	92.67	93.92	94.41	94.77	94.97	95.10	95.18	95.30	95.31	95.50	95.55	95.56	95.63	92.28
		GRSC	66.57	84.27	84.85	86.53	87.38	86.78	87.20	88.28	88.26	88.75	89.21	89.05	88.92	88.81	89.06	86.26
		MGSR	67.91	73.01	75.17	76.82	79.33	82.69	83.21	85.25	85.60	85.57	87.14	87.60	87.97	87.63	87.45	82.16
SA	KNN	SS-EMT	95.08	99.21	99.40	99.45	99.48	99.48	99.49	99.48	99.51	99.51	99.51	99.51	99.51	99.50	99.53	99.18
		GRSC	80.68	86.52	87.77	88.85	88.99	88.73	89.34	89.74	89.15	89.16	89.29	89.25	89.22	89.03	89.35	88.34
		MGSR	67.21	77.54	79.82	81.37	82.46	83.48	84.09	84.16	85.31	85.24	85.54	85.46	86.80	87.12	87.19	82.85
	SVM	SS-EMT	94.48	99.30	99.49	99.57	99.61	99.62	99.64	99.65	99.67	99.69	99.70	99.70	99.70	99.70	99.73	99.28
		GRSC	80.96	88.49	89.59	90.77	91.28	91.47	91.81	92.13	91.91	91.98	92.28	92.20	92.23	92.29	92.53	90.79
		MGSR	69.49	76.97	80.88	82.73	83.95	85.43	85.80	86.06	87.77	87.82	88.23	88.46	89.95	90.10	90.27	84.93
	RF	SS-EMT	94.84	99.25	99.42	99.49	99.53	99.52	99.54	99.52	99.56	99.55	99.57	99.56	99.55	99.56	99.55	99.20
		GRSC	80.96	88.41	88.82	89.99	90.09	90.16	90.93	90.66	90.73	90.62	90.69	90.46	90.57	90.59	90.59	89.62
		MGSR	67.71	67.21	77.54	79.82	81.37	82.46	83.48	84.09	84.16	85.31	85.24	85.54	85.46	86.80	87.12	81.55
BW	KNN	SS-EMT	74.78	88.53	91.56	92.00	92.45	93.16	94.16	94.11	94.03	94.47	94.35	94.35	94.61	94.07	94.77	92.09
		GRSC	57.36	60.06	60.25	62.07	61.68	61.60	62.68	62.37	64.26	76.54	77.79	77.46	78.12	79.11	78.58	68.00
		MGSR	36.19	67.41	73.95	76.16	77.64	78.78	79.29	78.93	79.65	81.55	81.97	82.67	82.69	82.67	85.02	76.30
	SVM	SS-EMT	74.19	90.34	92.96	93.46	94.06	94.63	95.03	95.43	95.31	95.08	95.64	95.91	95.67	95.92	96.37	93.33
		GRSC	64.53	67.00	67.27	67.54	68.20	71.67	69.70	70.43	79.30	82.16	83.89	84.44	84.21	85.47	84.90	75.38
		MGSR	42.30	70.26	79.94	81.75	83.28	84.68	85.08	84.72	84.71	88.51	88.56	88.40	87.70	87.27	89.60	81.79
	RF	SS-EMT	75.27	88.66	91.39	91.26	92.31	92.82	93.00	93.28	93.32	93.79	93.48	94.19	93.59	93.30	93.89	91.57
		GRSC	56.86	58.64	61.76	61.53	60.87	61.60	60.83	58.94	75.13	79.22	79.08	80.49	80.26	79.72	79.26	68.95
		MGSR	36.73	36.19	67.41	73.95	76.16	77.64	78.83	79.29	78.93	79.65	81.55	81.97	82.67	82.69	82.67	73.08

TABLE S-6: The KAPPA results of SS-EMT and two recent state-of-the-art FS methods on four datasets under three classifiers.

Dataset	Classifier	Algorithm	2	4	6	8	10	12	14	16	18	20	22	24	26	28	30	Mean	
IP	KNN	SS-EMT	0.744	0.856	0.879	0.888	0.895	0.898	0.900	0.902	0.905	0.906	0.907	0.905	0.907	0.910	0.908	0.887	
		GRSC	0.350	0.627	0.657	0.660	0.665	0.691	0.697	0.687	0.689	0.667	0.681	0.667	0.674	0.685	0.675	0.651	
		MGRS	0.149	0.357	0.435	0.469	0.468	0.540	0.552	0.555	0.572	0.572	0.584	0.595	0.594	0.603	0.601	0.510	
	SVM	SS-EMT	0.626	0.846	0.887	0.902	0.913	0.918	0.918	0.919	0.923	0.922	0.923	0.926	0.926	0.925	0.926	0.893	
		GRSC	0.309	0.610	0.658	0.689	0.730	0.765	0.764	0.798	0.795	0.773	0.788	0.767	0.769	0.784	0.789	0.719	
		MGRS	0.212	0.365	0.430	0.471	0.475	0.534	0.545	0.559	0.577	0.594	0.605	0.620	0.624	0.637	0.642	0.526	
	RF	SS-EMT	0.736	0.856	0.881	0.888	0.897	0.901	0.901	0.904	0.907	0.907	0.907	0.908	0.909	0.909	0.911	0.888	
		GRSC	0.352	0.642	0.652	0.664	0.691	0.699	0.695	0.716	0.729	0.694	0.713	0.700	0.707	0.697	0.712	0.671	
		MGRS	0.168	0.374	0.458	0.490	0.480	0.545	0.548	0.558	0.563	0.568	0.567	0.581	0.581	0.583	0.595	0.511	
PU	KNN	SS-EMT	0.475	0.751	0.856	0.900	0.919	0.926	0.932	0.936	0.938	0.939	0.941	0.941	0.942	0.942	0.942	0.885	
		GRSC	0.554	0.778	0.791	0.816	0.833	0.835	0.813	0.831	0.836	0.842	0.844	0.848	0.848	0.838	0.855	0.809	
		MGRS	0.572	0.621	0.650	0.676	0.714	0.769	0.778	0.808	0.811	0.813	0.833	0.844	0.842	0.844	0.841	0.761	
	SVM	SS-EMT	0.512	0.773	0.874	0.911	0.927	0.933	0.939	0.942	0.944	0.947	0.950	0.952	0.954	0.955	0.956	0.898	
		GRSC	0.598	0.768	0.789	0.840	0.868	0.861	0.873	0.889	0.894	0.901	0.902	0.901	0.902	0.903	0.908	0.853	
		MGRS	0.617	0.649	0.668	0.704	0.738	0.795	0.806	0.823	0.825	0.833	0.852	0.859	0.863	0.863	0.863	0.784	
	RF	SS-EMT	0.466	0.756	0.852	0.893	0.913	0.921	0.927	0.932	0.934	0.935	0.936	0.937	0.938	0.938	0.939	0.881	
		GRSC	0.550	0.788	0.796	0.818	0.830	0.822	0.828	0.842	0.842	0.848	0.855	0.852	0.851	0.849	0.853	0.815	
		MGRS	0.566	0.632	0.662	0.684	0.719	0.766	0.773	0.801	0.806	0.805	0.827	0.833	0.838	0.834	0.831	0.758	
SA	KNN	SS-EMT	0.835	0.984	0.991	0.993	0.994	0.994	0.994	0.994	0.994	0.994	0.994	0.994	0.994	0.994	0.995	0.983	
		GRSC	0.785	0.850	0.864	0.876	0.877	0.874	0.881	0.886	0.879	0.879	0.881	0.880	0.880	0.878	0.881	0.870	
		MGRS	0.628	0.749	0.775	0.792	0.804	0.816	0.823	0.824	0.836	0.836	0.839	0.838	0.853	0.857	0.857	0.808	
	SVM	SS-EMT	0.796	0.983	0.992	0.994	0.995	0.996	0.996	0.996	0.996	0.997	0.997	0.997	0.997	0.997	0.997	0.982	
		GRSC	0.786	0.871	0.884	0.897	0.903	0.905	0.909	0.912	0.910	0.910	0.914	0.913	0.913	0.914	0.917	0.897	
		MGRS	0.654	0.740	0.785	0.806	0.820	0.837	0.841	0.844	0.863	0.864	0.868	0.871	0.888	0.889	0.891	0.831	
	RF	SS-EMT	0.839	0.984	0.991	0.993	0.994	0.994	0.995	0.995	0.995	0.995	0.995	0.995	0.995	0.995	0.995	0.983	
		GRSC	0.788	0.871	0.876	0.889	0.890	0.891	0.899	0.896	0.897	0.896	0.896	0.894	0.895	0.895	0.895	0.884	
		MGRS	0.639	0.765	0.793	0.810	0.817	0.834	0.839	0.841	0.858	0.858	0.858	0.858	0.871	0.874	0.872	0.826	
BW	KNN	SS-EMT	0.640	0.864	0.904	0.919	0.930	0.933	0.936	0.938	0.940	0.945	0.944	0.945	0.948	0.949	0.945	0.912	
		GRSC	0.539	0.568	0.570	0.590	0.585	0.585	0.596	0.593	0.613	0.746	0.760	0.756	0.763	0.774	0.768	0.654	
		MGRS	0.310	0.647	0.718	0.742	0.758	0.770	0.776	0.772	0.780	0.800	0.805	0.812	0.813	0.812	0.838	0.743	
	SVM	SS-EMT	0.622	0.875	0.923	0.937	0.945	0.949	0.952	0.954	0.957	0.959	0.962	0.962	0.962	0.969	0.966	0.966	0.927
		GRSC	0.616	0.643	0.646	0.648	0.655	0.693	0.672	0.680	0.776	0.807	0.826	0.831	0.829	0.843	0.836	0.733	
		MGRS	0.374	0.678	0.783	0.802	0.819	0.834	0.838	0.834	0.834	0.876	0.876	0.874	0.867	0.862	0.887	0.803	
	RF	SS-EMT	0.634	0.861	0.898	0.910	0.921	0.927	0.930	0.930	0.930	0.933	0.937	0.937	0.933	0.938	0.935	0.938	0.904
		GRSC	0.533	0.552	0.586	0.583	0.576	0.584	0.576	0.555	0.731	0.775	0.774	0.789	0.786	0.780	0.775	0.664	
		MGRS	0.315	0.640	0.703	0.723	0.737	0.735	0.739	0.740	0.746	0.770	0.776	0.776	0.769	0.773	0.798	0.716	



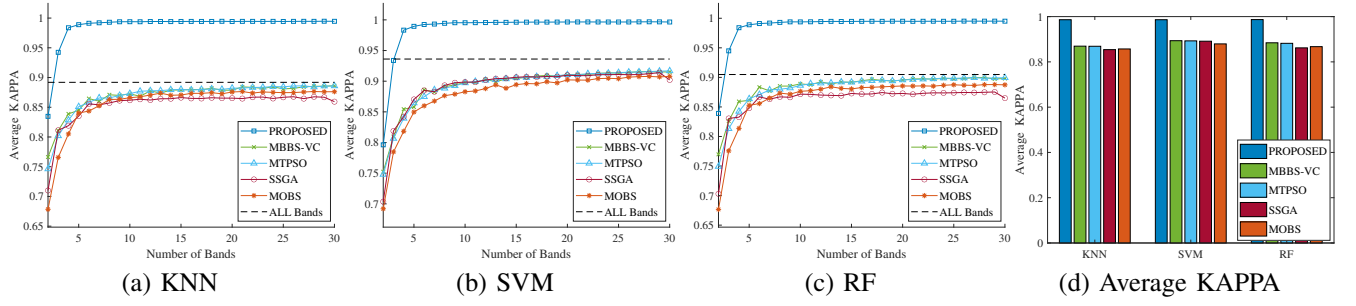


Fig. S-11: KAPPA coefficient results of SS-EMT and four EA-based FS methods on the Salinas dataset.

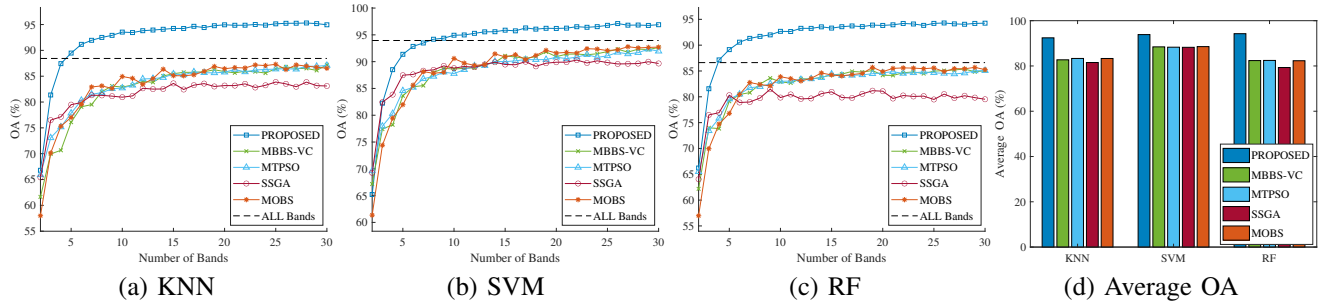


Fig. S-12: OA results of SS-EMT and four EA-based FS methods on the Bostwana dataset.

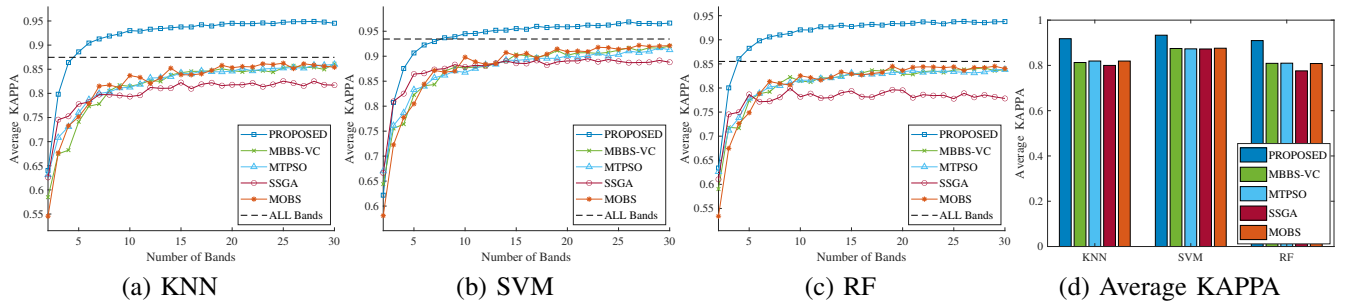


Fig. S-13: KAPPA coefficient results of SS-EMT and four EA-based FS methods on the Bostwana dataset.



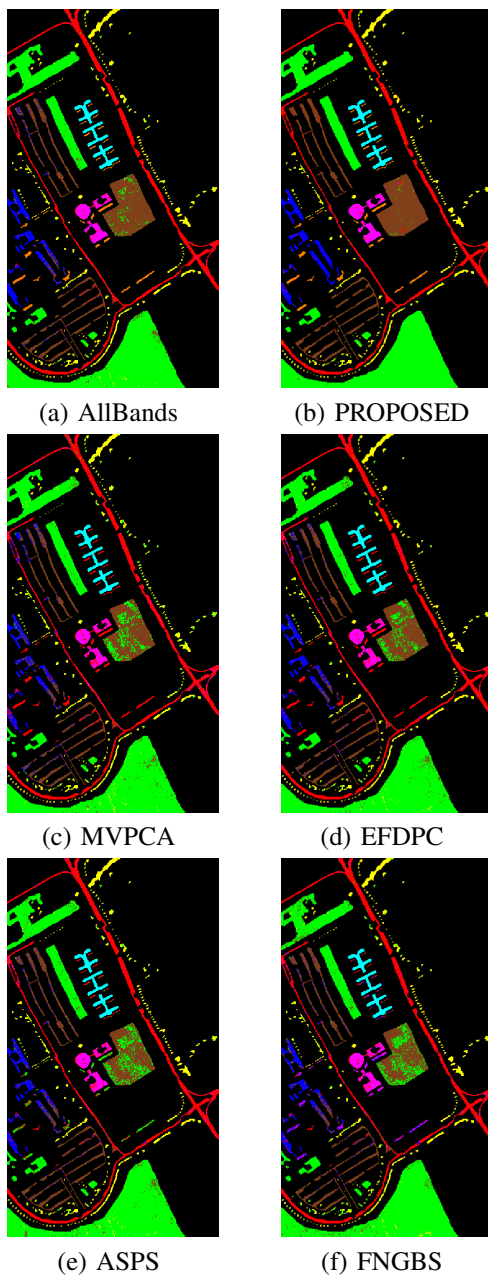


Fig. S-14: The classification maps of SS-EMT and four non-EA-based FS methods on the Pavia University dataset

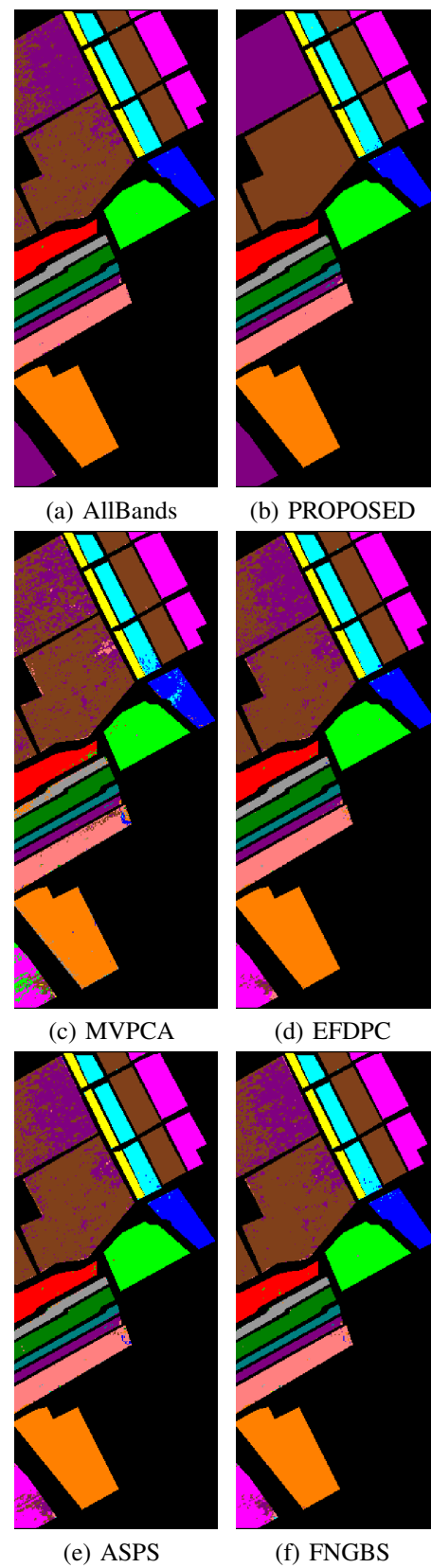


Fig. S-15: The classification maps of SS-EMT and four non-EA-based FS methods on the Salinas dataset

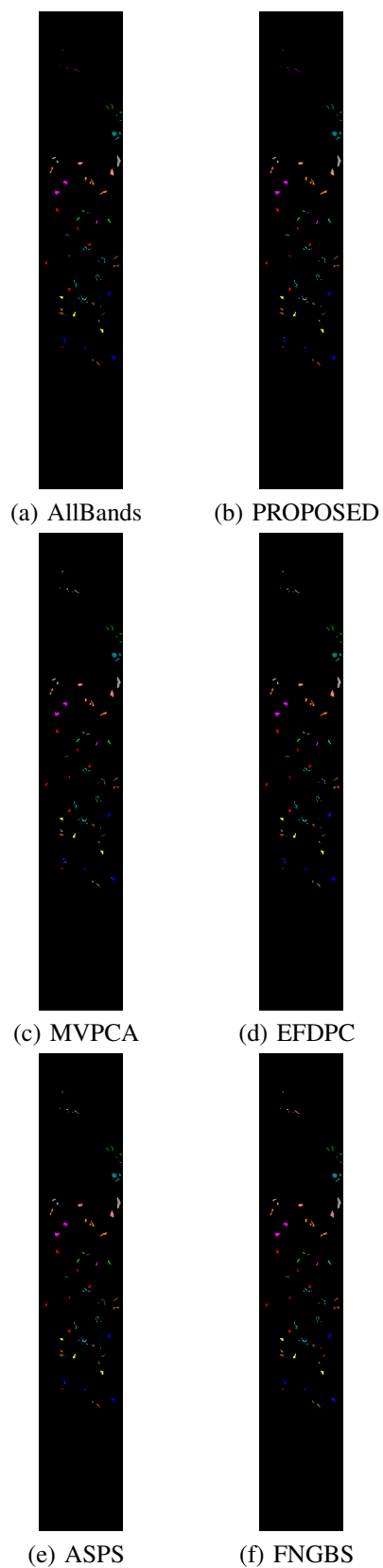


Fig. S-16: The classification maps of SS-EMT and four non-EA-based FS methods on the Bostwana dataset

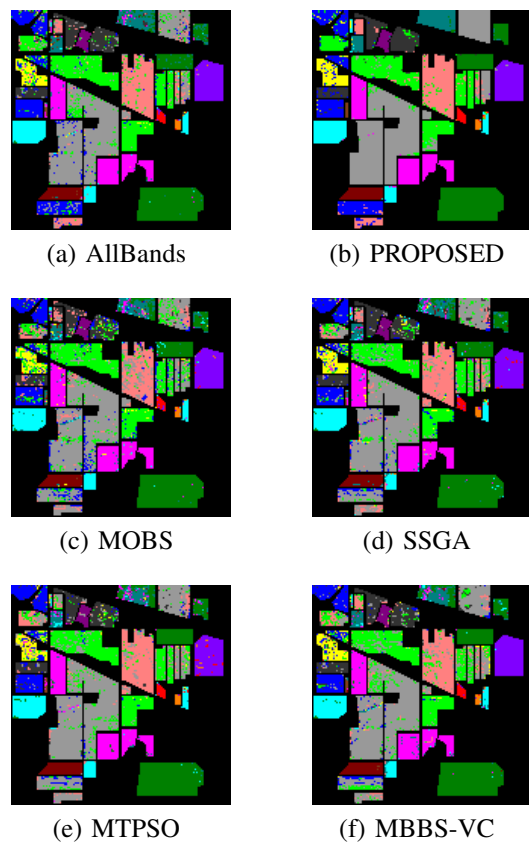


Fig. S-17: The classification maps of SS-EMT and four EA-based FS methods on the India Pines dataset.

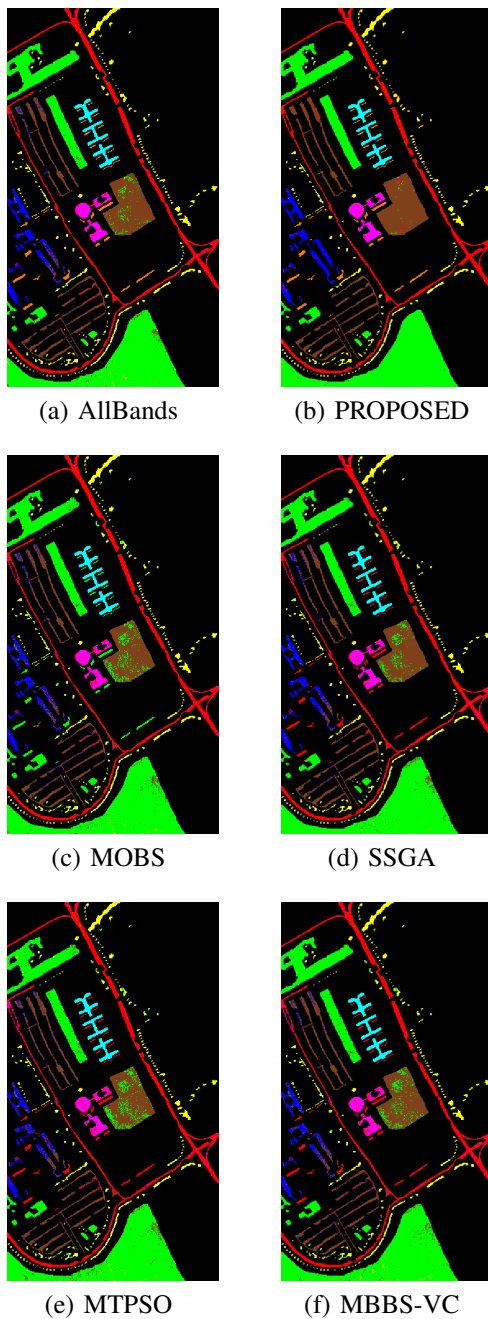


Fig. S-18: The classification maps of SS-EMT and four EA-based FS methods on the Pavia University dataset.

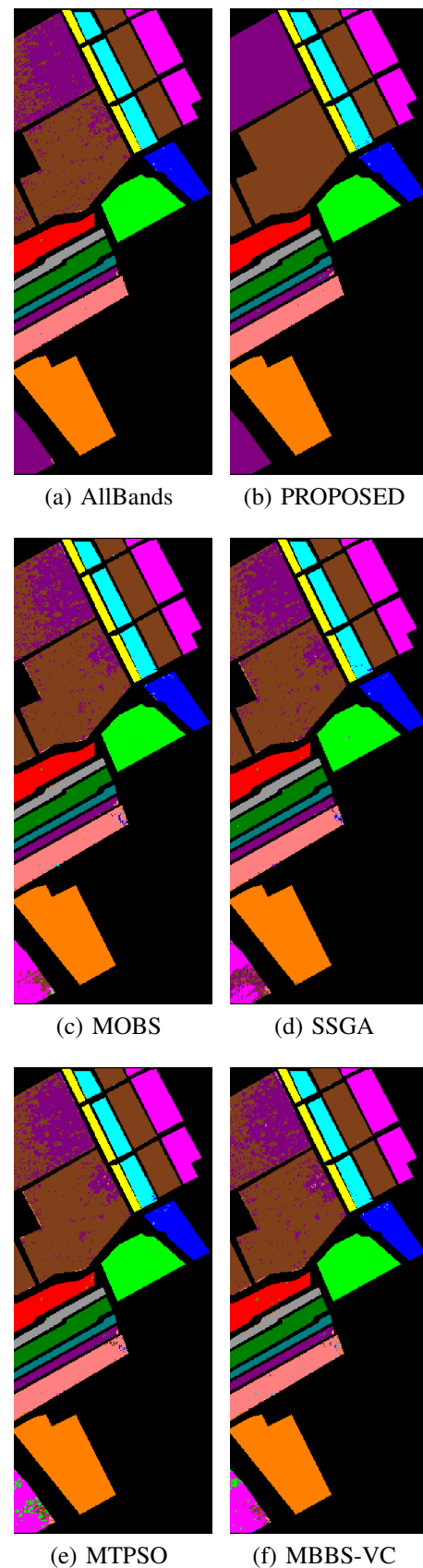


Fig. S-19: The classification maps of SS-EMT and four EA-based FS methods on the Salinas dataset.



Fig. S-20: The classification maps of SS-EMT and four EA-based FS methods on the Bostwana dataset.